High-accuracy determination of epitaxial AlGaAs composition with inductively coupled plasma optical emission spectroscopy

K. A. Bertness[a)] and C. M. Wang
National Institute of Standards and Technology, Mail Stop 815.04, 325 Broadway, Boulder, Colorado 80305

M. L. Salit, G. C. Turk, T. A. Butler, A. J. Paul, and L. H. Robins
National Institute of Standards and Technology, 100 Bureau Drive, Gaithersburg, Maryland 20899

Inductively coupled plasma optical emission spectroscopy is shown to confirm a recent correlation between photoluminescence (PL) peak energy for AlGaAs epitaxial films and the Al mole fraction x of those films. These two methods also agree within their expanded uncertainties with the Al composition as determined by growth rate measurements using reflection high energy electron diffraction intensity at the time of specimen growth. No systematic variations between the three methods as a function of Al mole fraction were observed. The lowest uncertainty was found in the PL measurements, allowing certification of Al mole fraction x in standard reference materials to an expanded uncertainty of 0.003 for $x < 0.35$. Details of the uncertainty analysis, as well as possible improvements in those uncertainties, are discussed. [DOI: 10.1116/1.2181579]

I. INTRODUCTION

We have applied a high-performance analytical chemistry method, inductively coupled plasma optical emission spectroscopy (ICP-OES), to the measurement of the composition of AlGaAs epitaxial layers in order to facilitate the placement of the more routine analysis methods on a composition scale with a complete uncertainty estimate and unambiguous traceability to the mole. ICP-OES measurements of epitaxial layer samples were compared with measurements of standards prepared from well-characterized high-purity solids. For this work, AlGaAs standards were prepared as a mixture of single-element solution standard reference materials (SRMs) from NIST.[1] Measurements reported herein are traceable to these standards, which are traceable to the international system of units (SI).

Using the conventional definition of Al mole fraction x in $Al_xGa_{1-x}As$, ICP-OES compositions have been obtained with an expanded uncertainty of 0.006 or less in x for films with x from 0.10 to 0.35. The composition measurements have been compared with compositions determined from photoluminescence (PL) peak energy and reflection high energy electron diffraction (RHEED) growth rate measurements at the time of specimen growth. All three measurements agree within their expanded uncertainties. (Unless otherwise noted, all of the uncertainty values given in this paper are expanded uncertainties, or 2σ, values equal to twice the standard uncertainty, or 1σ value, for a 95% confidence interval.) The data obtained in this experiment thus provide strong additional confirmation of the PL techniques for correlating the composition with PL peak energy E_{PL} as outlined in a recent paper by Robins *et al.*[2] In that paper, the best correlation between E_{PL} and Al mole fraction was obtained with the equation $x = (0.7134 \pm 0.0046\ \text{eV}^{-1}) \cdot (E_{PL}$

$- 1.423\ 26 \pm 0.000\ 47\ \text{eV})$. The coefficients in this equation differ from many commonly used values. The best previous measurements of the calibration coefficients were based on nuclear resonant reaction analysis.[3] The ICP-OES method has the advantage of being extendable to a number of alloy systems that are not accessible with nuclear reaction methods.

This work has been undertaken to establish a foundation for the production and certification of Al mole fraction SRMs consisting of AlGaAs epitaxial layers on GaAs with the mole fraction certified to an uncertainty of 0.003. A number of certification methods have been examined, and PL has proven to be a nondestructive, repeatable method with high relative precision. The difficulty in applying PL to composition measurement has been the lack of traceable calibrant materials and the sensitivity to noncompositional specimen characteristics, chiefly specimen doping level and temperature. Temperature in this context also includes local heating from the laser beam used to excite the luminescence. The constraints are thus somewhat conflicting, because PL intensity in bulk layers increases with doping level, reducing the need for high excitation power, while even moderately high doping shifts the PL peak energy. We have established that doping concentrations in the low $10^{16}\ \text{cm}^{-3}$ range generally give a good compromise between high PL intensity at low excitation power without significant peak shift from the doping itself. Although the SRMs will necessarily be lower in doping concentration than many epitaxial layers used in practical applications, the SRMs can be used to calibrate secondary references consisting of epitaxial layers with higher doping. The traceability chain between the SRMs and secondary references will require measurement methods that are insensitive to doping level, such as electron microprobe analysis or x-ray photoemission spectroscopy.

In ICP-OES, the analyte must be in solution form. The test is necessarily destructive of the film and has its primary

[a)]Electronic mail: bertness@boulder.nist.gov

value for this application in placing other methods on a traceable, absolute composition scale. It is also immune to most environmental and specimen secondary effects, such as sample doping, strain, and temperature. As described below, the films were dissolved from the substrate with an acid solution. In order to avoid contamination of the solutions from GaAs substrates, the specimens used in this study were grown on Ge substrates. The actual Al mole fraction SRMs will incorporate GaAs substrates and be certified with PL and RHEED. Although not explored in these experiments, methods also exist for removing part of the film without etching down to the substrate, so the substrate limitation is not a universal one. As we will show, PL has the highest demonstrated precision of the three methods. With additional improvements and additional specimens, the ICP-OES method would provide a more stringent test of the PL calibration than has previously been possible.

II. EXPERIMENT DESCRIPTION

A. Overview of ICP-OES procedures

In these ICP-OES experiments, a solution containing the elements to be analyzed was injected into a plasma, causing excitation of optical emission lines. In so far as appropriate, we used previously developed methods[4] for high performance in ICP-OES. For this experiment, the emission lines monitored were 396.153 nm for Al, 193.696 nm for As, and either 294.364 or 417.206 nm for Ga. Although the data were analyzed using element ratios, e.g., Al/Ga, rather than absolute mass concentrations, the method of spiking with additional elements described in Ref. 4 was not used. Calibrant solutions were mixtures of single-element spectrometric solutions issued as NIST SRMs with certified mass fractions, and their preparation is described in more detail below. In a single ICP-OES run, there were typically 12 calibrants, two unknown mixtures (from neighboring pieces of the same wafer), and a "blank" solution of dilute nitric acid. The ICP-OES instrument was equipped with an autosampler that mechanically moves the inlet tube from one specimen tube to the next in a fixed pattern. The volume of solution consumed in each sampling was approximately 3 ml, and each solution was sampled five times in each ICP-OES run. Within each sampling, five detector readings were obtained for each element, and these readings were averaged by element. The blank solution was used to provide a background subtraction correction for the counts of each individual element. Background corrections were on the order of 0.5%–1% of the total signal count. The signals from individual elements were then used to calculate the ratios Al/As, Al/Ga, and Ga/As for each sampling. A drift correction procedure, described in more detail below, was applied to the individual ratios. The data on the calibrants were used to compute a calibration coefficient for the unknowns, using a simple linear dependence $R_s = \langle C_s \rangle S$, where R_s is the measurement result for elemental ratio in the unknown specimen, C_s is the count ratio for the unknown specimen, and S is the calibration coefficient. The use of a linear model with zero intercept is justi-

fied by subtracting the spectral background and by diluting the reference solutions so that the absolute element intensities were within about 20% of the intensities for the unknown solutions.

The calibration coefficient S was computed by averaging the ratio of the elements in the calibrant solutions R_c, which is known from the preparation process, and the actual count ratios C_c for the calibrants in the current ICP-OES run, that is, $S = (R_c/C_c)_{\mathrm{avg}}$. A different S value was needed for each elemental ratio. The uncertainty was reduced by averaging over the appropriate number of calibrant solutions. As discussed below, the calibrants without any added sulfuric solution were shown to be the best predictors of the true values, and therefore S was set to the average over the four calibrants in each run that did not contain sulfuric solution. The uncertainty in S had two components: the uncertainty inherited from the original parent solutions and the uncertainty associated with mixing and measuring the solutions in ICP-OES. Because these two sources of error can safely be assumed to be uncorrelated, the final uncertainty in S, u_S, is given by $u_S = S[(u_R/R)^2 + (u_{C_c}/\langle C_c \rangle)^2]^{1/2}$, where R represents the calculated ratio for the calibrant solutions; u_R is the uncertainty in those ratios propagated from the uncertainty in the parent solutions; u_{C_c} is the uncertainty of the mean, derived from twice the standard deviation of the distribution across the four calibrant solutions divided by the square root of the number of the solutions; and $\langle C_c \rangle$ is the mean of the count ratios in the measurements of those solutions.

The elemental ratios derived from ICP-OES were then combined to calculate the mole fraction x for the film by using the following three different equations:

$$x_a = \mathrm{Al/As}, \tag{1}$$

$$x_b = (\mathrm{Al/Ga})/[1 + (\mathrm{Al/Ga})], \tag{2}$$

$$x_g = 1 - (\mathrm{Ga/As}). \tag{3}$$

These equations are equivalent, based on the well-established property of conventionally grown GaAs and related alloys that the sum of the atomic fraction of the group III elements (here Al and Ga) is equal to the atomic fraction of the group V element to within a factor of better than 1.0002.[5,6] This property arises from the high formation energy of antisite defects and interstitials in this crystal structure. If all sources of uncertainty and bias are included, the three determinations of mole fraction should agree within their calculated expanded uncertainties. It should be noted that an adjustment factor in the As calibration can always be found that will produce agreement among the three equations. The test of the method thus comes from agreement within the calculated uncertainties, and not the selection of calibration coefficients that produce agreement. As will be discussed further below, we did observe evidence of bias in some of the measurements, and selected x_a and x_g for combination into a single best estimate of x.

B. Unknown AlGaAs layer specimen preparation

The epitaxial layer specimens were grown with molecular beam epitaxy on Ge substrates. The layers were homogeneous in composition at a single Al mole fraction for a total thickness of 3 μm. RHEED measurements of the Al and Ga flux before and after the growth runs were used as one determination of the film mole fraction.[7] Film homogeneity is supported by the continuity of flux measurements before and after a run, by the lateral uniformity in PL measurements (discussed further below), and by secondary-ion-mass spectrometry (SIMS) profiles. SIMS profiles set an upper limit of 1.2% on the relative variation of the Al mole fraction with film depth. Growth of smooth, uniform films was accomplished by using epiready Ge (100) wafers miscut 6° toward ⟨111⟩ and a multistage, low-temperature buffer layer. The substrates were prepared for growth by heating in vacuum to approximately 480 °C, as measured by an optical pyrometer, where the oxide first began to desorb. The substrates were heated further to approximately 550 °C to ensure complete oxide removal and a stable, streaky RHEED pattern. The substrates were then cooled to 380±30 °C, and growth was initiated with simultaneous pulses of Al and Ga alternating with pulses of As to promote surface diffusion. After approximately 10 nm of growth, the substrate temperature was increased by 50 °C and pulses of AlGaAs were alternated with growth pauses under As flux until another 15 nm had been deposited. This process was repeated at three additional temperatures (490, 535, and 545±10 °C) for 5 nm of pulsed deposition at each stage. The remaining 2.96 μm of the AlGaAs layer was grown continuously at a growth temperature of 555 °C and a growth rate of approximately 0.3 nm/s. The layers were doped with Si such that the free carrier concentration was between 1×10^{16} and 2×10^{16} cm^{-3}.

After removal from the growth chamber, the front side of the wafer was coated with photoresist to allow etching of the backside to remove any deposits accumulated during growth. The photoresist also protected the wafers while they were diced into 1×1 cm^2 pieces. Neighboring pieces taken from the wafer center were analyzed with PL and ICP-OES. ICP-OES unknown solutions were obtained from the epitaxial AlGaAs layers by etching a single 1×1 cm^2 piece with a 4:1:1 mixture of H_2SO_4:H_2O_2:H_2O. The etch solution was administered with a pipette that was weighed before and after several drops were placed upon the surface. The net weight of the etchant varied from 20 to 40 mg for this experiment series. The specimens underwent a slight change in color when the AlGaAs film was mostly dissolved; to ensure complete removal, the etching was allowed to continue for a few minutes past the color change. The specimen was then flooded with a dilute nitric acid solution to reach a total solution mass of approximately 50 g, and the substrate was removed from the solution. The solution was then transferred into a polypropylene bottle for storage until analysis time. Representative specimens were analyzed with SIMS to exclude the possibility that solutions might be biased by differential interdiffusion at the Ge–AlGaAs interface. The SIMS data indicated that interdiffusion could have altered the mass

TABLE I. SRM specifications for parent ICP-OES solutions used in this experiment.

SRM number and element	Lot	Concentration and expanded uncertainty (mg/g)	Fractional uncertainty (expanded)
3101a Al	010808	9.999±0.036	0.0036
3119a Ga	890709	10.00±0.04	0.0040
3103a As	010713	9.941±0.055	0.0055

of the layer contributed by each constituent by only a fraction less than 3×10^{-5}, and therefore could be ignored. The solution specimens were likely to vary in the quantity of Ge included. The absolute mass of Al, Ga, and As in the unknown solutions was approximately 0.06, 0.6, and 0.8 mg, respectively, for the $x=0.20$ layers.

C. ICP-OES calibrant preparation

Calibrants were generated by mixing SRM solutions (see Table I) for individual elements and dilute HNO_3 to approximately the same ratios expected in the unknowns. The Al SRM underwent an initial 10:1 dilution with dilute HNO_3 to reduce its concentration to enable easier matching to the unknowns. A set of four different standard mixtures, denoted by letters A–D, were generated for each nominal Al mole fraction under test: 0.10, 0.185, 0.30, and 0.35. In order to determine whether or not the sulfuric acid etchant used on the AlGaAs epilayers would bias the measurements, referred to as the "matrix effect," additional calibrants were also generated by adding a weighed amount of sulfuric etchant to the calibrants. The sulfuric etchant was added at the time of the ICP-OES run to the sample vials of the autosampler. Most of the data were obtained with additional dilution of the calibrant solutions so that the absolute value of the individual element counts would be within 20% of that in the unknowns. This final dilution took place in the sample tubes of the autosampler. The apparent elemental ratio in the calibrants without sulfuric etchant differed by a factor no greater than 1.003 relative to the calibrants with etchant at a similar concentration to that used in the unknowns. The matrix effect was strongest at etchant concentrations *below* those present in the unknown solutions, and was roughly similar for Ga/As and Al/As ratios, with no consistent effect on the Al/Ga ratio. The behavior suggests that there may be some shifts in the oxidation state of the As in solution, and this can have a slight but measurable effect on the sensitivity of ICP-OES to As.[8] Nevertheless, because the matrix effect was small and dominated by noise, we omitted any deliberate correction. The calibration coefficients were therefore calculated from the data on the subset of calibrant solutions that did not contain a sulfuric etchant.

D. Drift correction procedure

Many noise sources in ICP-OES are correlated among elements, and therefore their effect on the composition analysis can be reduced by taking ratios of elements for the
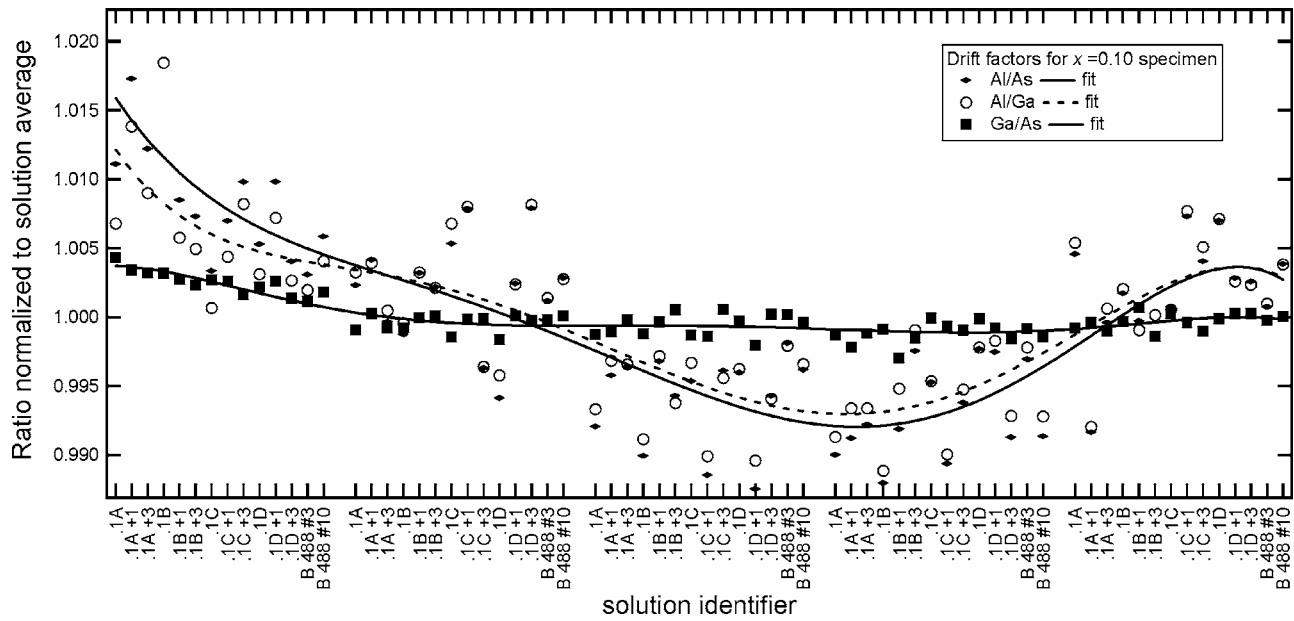
FIG. 1. Drift correction procedure illustration. Solution identifiers beginning with the letter "B" are unknowns; the rest are the various calibrants with different degrees of spiking with the sulfuric etchant.

data acquired at approximately the same time. Biases due to longer term drift can also be mitigated by applying a drift correction.[9] As described above, each solution was sampled five times as part of the complete ICP-OES run. The element ratios for each solution were averaged, and then the individual ratios were normalized to the average for that element combination and solution. The data were then plotted sequentially in the same order that they were acquired. An example is given in Fig. 1 for one of the runs on the $x = 0.10$ specimens. The data for each ratio (e.g., Al/As) were fitted with a seventh order polynomial, and this polynomial value was used to renormalize all of the data for that ratio. Long-term drift of the instrument was thus removed, while the short-term, uncorrelated noise remains. The data in Fig. 1 were fairly typical for the data in this experiment, where the noise in ratios containing Al was greater. The full range of drift corrections in this experiment varied from approximately 0.99 to 1.04. Because of the small absolute range of the drift, and the use of averaging over the five samplings, adding a drift correction had little effect on the final determination of the mole fraction. The drift correction shift never exceeded the standard uncertainty for the mole fraction results, ranging from 2% to 15% of the expanded uncertainty.

III. DATA AND DISCUSSION

Following the procedures described above, pieces from each of five growth runs were evaluated with RHEED, PL, and ICP-OES. The results of these measurements are summarized in Table II along with the standard uncertainty values. By virtue of the experimental procedure, the measurement of x with RHEED applies to the entire central region of the wafer. The PL data were acquired on 1×1 cm^2 specimens located adjacent to the ICP-OES specimens on the original wafer, and the PL uncertainty estimate includes any

variation over 12 separate locations on the specimen. Spatial variations in composition from wafers grown in this growth system have been examined for a number of runs, and the variation in x over a distance of about 1 cm has always been smaller than 0.0005, and more typically less than 0.0002. At least two ICP-OES specimens were analyzed from each wafer. The ICP-OES data from multiple specimens and multiple specimen runs (repeated runs with the same unknown solutions) were combined using a weighted mean. Because the uncertainty in the ICP-OES data included the uncertainty of the parent solutions, a quantity that is highly correlated for all the ICP-OES runs, the uncertainty in the mean was calculated from an upper limit for the highly correlated data. Specifically, the overall uncertainty was the sum of the weighted uncertainties of the individual measurements, where the weighting factor for the ith uncertainty contribution is $(1/u_i^2)/\Sigma(1/u_j^2)$, the same factor that is used for the weighted mean itself.

In Fig. 2 the data are plotted as the deviation from the mole fraction as determined from PL, the method with the smallest uncertainty. From this plot, we see that there is agreement between all three methods within the expanded

TABLE II. Comparison of Al mole fraction x and expanded uncertainty (2σ) for various AlGaAs specimens as determined by RHEED, PL, and ICP-OES.

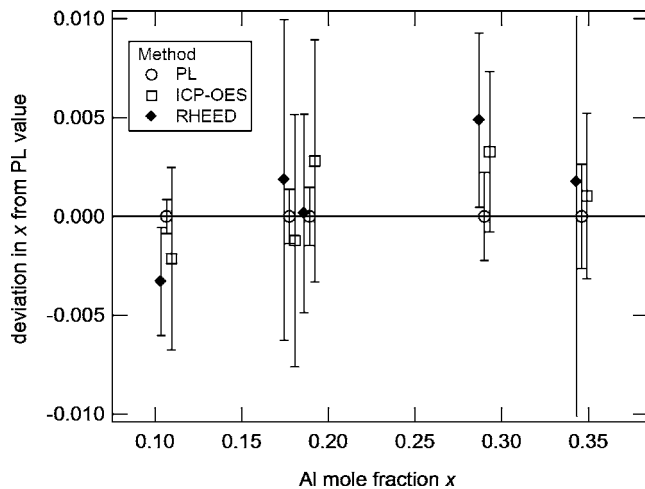| Name	x_{RHEED}	2σ	x_{PL}	2σ	$x_{\text{ICP-OES}}$	2σ
B488	0.1032	0.0026	0.1062	0.000 87	0.1044	0.0045
B489	0.1794	0.0080	0.1773	0.001 38	0.1763	0.0062
B486	0.1893	0.0048	0.1889	0.001 47	0.1920	0.0059
B485	0.2950	0.0038	0.2899	0.002 22	0.2934	0.0034
B490	0.3480	0.0120	0.3460	0.002 64	0.3473	0.0033

FIG. 2. Deviation in Al mole fraction x from the value determined with PL for the wafers listed in Table II. The ICP-OES and RHEED data have been shifted horizontally to the right and left, respectively, for greater clarity. The uncertainty bars represent the expanded uncertainty (2σ).

and in being able to accurately locate the center of the substrate. Low-frequency vibrations from pumping systems, particularly cryopumps, can degrade the accuracy of the RHEED intensity data if the substrate is not securely mounted. Unfortunately, most indium-free substrate holders for small specimens allow both vibration and tilting of the specimens. In subsequent experiments we have been able to reduce the uncertainty in the RHEED mole fraction determination to between 0.004 and 0.006 expanded uncertainty, and although this is an improvement for two of the six specimens in this study, further improvements are unlikely to be possible.

The ICP-OES data present more opportunities for higher accuracy. Data on the unknowns for a typical run are illustrated in Fig. 3(a), where x_a, x_b, and x_g are graphed for two specimens from the same wafer, B490. As for most of the ICP-OES data runs, the Al mole fraction x_b calculated from the Al/Ga ratio falls between the values derived from Al/As and Ga/As. This trend may be explained by the previously mentioned oxidation effect in the As SRM solutions. Controlling the oxidation state of As with a redox buffer should eliminate variability arising from this issue. Experimentally we observe that the sum of the Al/As and Ga/As ratios varies from 0.994 to 1.005 for most specimens.

The ultimate limit to the accuracy of the assessment comes from the parent solutions used to generate the calibrant solutions. In Table III, the uncertainty contribution from the parent solutions is calculated for two values of x. The contribution from the parent solutions is the minimum uncertainty we can expect from this method, and it can be achieved only when all other sources of uncertainty are negligible. Although the fractional uncertainties for each element are similar in the parent solutions, the skewing induced by the propagation of uncertainty to the mole fraction result predicts that the Al/Ga ratio will give the lowest final uncer-

uncertainties and that there are no systematic biases in one method as a function of mole fraction. The data in Table II and Fig. 2 show that we expect to be able to certify SRMs in the $x=0.2$ to $x=0.3$ range to a 0.002 expanded uncertainty. The RHEED measurements on SRMs can be used as a quality check on the PL measurements, and in part to sense shifts due to doping and temperature.

Although the data agree within their expanded uncertainties, the scatter and the stringency of the comparison could be improved with the reduction of those uncertainties. Our previous work on RHEED has shown that the uncertainty is limited by beam placement and acquisition to long periods where the signal is often noisy. Further work has shown that RHEED substrate mounting is a key factor in limiting noise
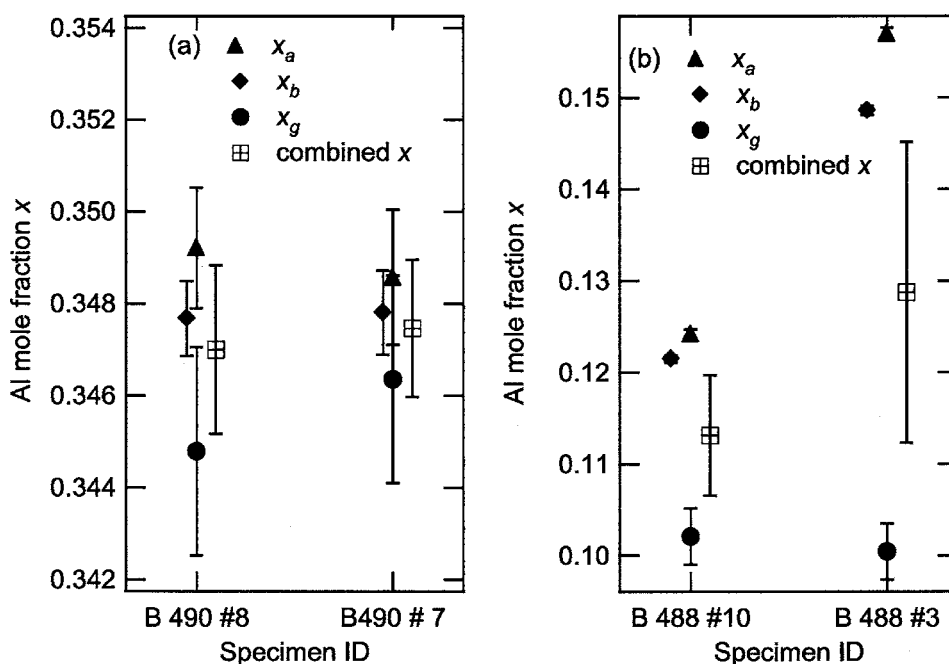

FIG. 3. Detailed analysis of specimens with (a) Al mole fraction $x \approx 0.35$ and (b) $x \approx 0.10$ with evidence for possible Al contamination. The Al mole fractions shown are calculated from three different ratios, Al/As, Al/Ga, and Ga/As, using Eqs. (1)–(3). Error bars represent the standard uncertainty (1σ).

TABLE III. Minimum fractional expanded uncertainty f for each element ratio and resulting minimum absolute uncertainty u_x in mole fraction x based on contribution of parent ICP-OES solutions to overall uncertainty. Also illustrated are the minimum expanded uncertainty for the consensus method, combination of the Al/As and Ga/As mole fraction derivations, and the equations used to calculate the minimum uncertainties.

Ratio R	Ratio fractional uncertainty f	Minimum u_x for $x \approx 0.20$	Minimum u_x for $x \approx 0.35$	Eq. for minimum u_x
Al/As	0.0066	0.0013	0.0023	xf
Al/Ga	0.0054	0.000 86	0.0012	$[x(1-x)]f$
Ga/As	0.0068	0.0054	0.0044	$(1-x)f$
Consensus		0.0028	0.0025	$(1/2)(u_{xa}^2 + u_{xg}^2)^{1/2}$

tainty when other experimental noise sources are moderate and similar for each element. Unfortunately, there were data sets such as those illustrated in Fig. 3(b). For these data sets, we observed that the mole fractions x_a, x_b, and x_g differed by substantially more than their estimated uncertainties. In particular, the Al-derived mole fractions x_a and x_b were high compared with x_g, and high compared with x as determined from RHEED and PL. The apparent explanation is that the Al signal was perturbed by either contamination or spectral interference. The Al 396.153 nm spectral line is known to overlap an OH emission band. This overlap is typically small in scale and typically corrected by background subtraction, but the potential for matrix variation in this experiment is significant. Changes in the solvent composition introduced to the plasma could cause significant change in the OH emission intensity at that wavelength.

Supporting the contamination theory was an observed increase in Al signal over time. The Al signal was much larger for unknown solutions that had been stored for two weeks than for solutions that were freshly made. One possible source of the Al was the storage bottles themselves, possibly enhanced by the presence of the sulfuric solution. The effect was observed only for the $x=0.10$ solutions, where the Al present was estimated at a mere 30 μg, although most solutions were not examined after long storage periods. Other possible explanations include chemical reactions or oxidation state changes involving Al that systematically shift the results, much like the oxidation effect in As analysis. The greater variability in the Al-containing ratios in the drift correction curves suggests some sort of chemical sensitivity effect for Al, though the magnitude of the variations in Fig. 1 (and the data for other specimens) was insufficient to explain the large shifts in x_a seen in Fig. 3(b). Because the source of the disagreement is still unknown, we applied a statistically rigorous consensus method of combining data that incorporates both the within-method uncertainties and a between-

method uncertainty.[10] We chose to combine x_a and x_g because the As oxidation effect tends to cancel in averaging these values. The consensus method results in a minimum uncertainty based on the parent solution contributions to u_a and u_g added in quadrature and then divided by two. For low Al mole fraction, this method therefore leads to a higher overall uncertainty in x through u_g than would be found from the adoption of the single-ratio derivation of x_b.

Identification of experimental conditions that eliminate the unusual spikes in x_a and that mitigate As oxidation effects would allow ICP-OES determination with uncertainties u_x on the order of 0.001, three to six times less than the uncertainties obtained in this experimental data set. This additional level of accuracy would allow better refinement of the PL calibration coefficients and resolution of nonlinear effects (if present) in the correlation of peak PL energy with Al mole fraction.

IV. CONCLUSIONS

ICP-OES has been shown to provide additional confirmation of the determination of the Al mole fraction in AlGaAs epitaxial films with photoluminescence peak energy. Both methods also agree with RHEED composition measurements within the expanded uncertainties of the methods. ICP-OES offers the advantages of being traceable to the mole and applicable to a number of epitaxial layer systems. The data sets examined here support the use of PL to certify the Al mole fraction x of AlGaAs epitaxial layers to an expanded uncertainty of 0.003 or less for $x<0.35$. The ICP-OES analysis was tested against the crystal properties of AlGaAs that assert that the sum of the Al and Ga atomic densities is equal to the As atomic density to much better than the analysis uncertainties. This extra check revealed anomalies in the Al concentration measurement that increased the uncertainty in the ICP-OES measurements by a factor of 3–6. Elimination of these anomalies will lead to uncertainty values that have the potential to increase the accuracy of the PL determination even further.

[1] Certificates of analysis for NIST SRM 3101a, A1 Standard Solution; NIST SRM 3103a, Arsenic Standard Solution; and NIST SRM 3119a, Gallium Standard Solution, http://www.nist.gov
[2] L. H. Robins, J. T. Armstrong, R. B. Marinenko, A. J. Paul, J. G. Pellegrino, and K. A. Bertness, J. Appl. Phys. **93**, 3747 (2003).
[3] T. F. Kuech *et al.*, Appl. Phys. Lett. **51**, 505 (1987).
[4] M. L. Salit, G. C. Turk, A. P. Lindstrom, T. A. Butler, C. M. Beck II, and B. Norman, Anal. Chem. **73**, 4821 (2001).
[5] L. Y. Lin, X. R. Zhong, and N. F. Chen, J. Cryst. Growth **191**, 586 (1998).
[6] N. Chen, Y. Wang, H. He, Z. Wang, L. Lin, and O. Oda, Appl. Phys. Lett. **69**, 3890 (1996).
[7] T. E. Harvey, K. A. Bertness, R. K. Hickernell, C. M. Wang, and J. D. Splett, J. Cryst. Growth **251**, 73 (2003).
[8] L. L. Yu (private communication).
[9] M. L. Salit and G. C. Turk, Anal. Chem. **70**, 3184 (1998).
[10] M. S. Levenson *et al.*, J. Res. Natl. Inst. Stand. Technol. **105**, 571 (2000).